The excitation of IF($B\,^3\Pi_{0^+}$) by $N_2(A\,^3\Sigma_u^+)$

L. G. Piper, W. J. Marinelli, W. T. Rawlins, and B. D. Green
Physical Sciences Inc., Research Park, P.O. Box 3100, Andover, Massachusetts 01810

(Received 7 August 1985; accepted 21 August 1985)

Experiments in a discharge-flow reactor show that the energy-transfer reaction between $N_2(A\,^3\Sigma_u^+)$ and $IF(X\,^1\Sigma^+)$ is extremely rapid ($k_{\text{total}} = 2.0\times10^{-10}$ cm^3 molecule^{-1} s^{-1}) with 40% of the quenching collisions resulting in fluorescence from $IF(B\,^3\Pi_{0^+})$. The reaction populates IF(B) vibrational levels up through $v' = 9$ and produces $v' = 0$–6 with about equal probability at low pressure. The vibrational distribution relaxes rapidly in collisions with the reactor bath gas even at pressures of a few Torr. The vibrational relaxation rate coefficients for levels 3–6 of IF(B) in a mixture of 80% Ar/20% N_2 are about 3×10^{-12} cm^3 molecule^{-1} s^{-1}, with levels 1 and 2 being a little slower. Differences in IF excitation between $N_2(A)$ $v' = 1$ and $v' = 0$ are small ($k_{v'=1}/k_{v'=0} \leqslant 1.2$). Electronic quenching of the IF(B) is sufficiently slow that even at higher reactor pressures radiative decay is the dominant loss. Rate coefficients for quenching $N_2(A)$, by CF_3I, and NF_3 and for vibrational relaxation of $N_2(A, v' = 1)$ by CF_4, CF_3H, CH_4, and SF_6 also are reported.

I. INTRODUCTION

The molecule IF and other interhalogens have been the subject of considerable interest in recent years because their compressed electronic energy manifold and intense radiative transitions cause these molecules to exhibit visible lasing action. The "blue-green" emission, $D'(^3\Pi_2) \rightarrow A'(^3\Pi_2)$, of IF has been studied extensively for application in short-wavelength, gas-discharge chemical lasers.[1]

Recently, interest has also focused on the $(B\,^3\Pi_{0^+}) \rightarrow X(^1\Sigma^+)$ bands of the interhalogens. In an elegant series of papers, Clyne and co-workers studied the radiative and collisional properties of IF and BrF. They showed that these species were highly suitable for forming an electronic transition laser operating on the $B \rightarrow X$ transition[2–7] because the upper states have short radiative and long quenching lifetimes. In parallel with this work, Davis and Hanko,[8] using a pulsed dye laser to excite the ground-state IF formed in an I_2/F_2 flame, demonstrated optically pumped lasing action on the IF($B \rightarrow X$) transition. Optimal chemical (kinetic) means for pumping the IF(B) state remain to be determined.

More than a decade ago, Clyne *et al.*[9] studied the three-body recombination of I with F, and noted extensive enhancement of the IF($B \rightarrow X$) emission upon adding $O_2(^1\Delta, ^1\Sigma)$ to the reacting mixture. Recently, Davis and co-workers[10] demonstrated and examined the enhancement of IF(B) emission from the I_2/F_2 system upon introducing $O_2(^1\Delta)$ and $O_2(^1\Sigma)$. In these experiments, $O_2(^1\Delta)$, rather than $O_2(^1\Sigma)$, appeared to be responsible for the IF(B) enhancement. In the absence of O_2^*, IF[$B(v)$] distributions were relatively cold, extending only to about $v' = 4$–5. Adding O_2^* greatly enhanced the $B \rightarrow X$ emission intensity, with up to ten vibrational quanta excited in the B state. Subsequent work by Davis and co-workers[11] shows even stronger IF(B) excitation when the effluents of microwave discharges in He/N_2 mixtures interact with the I_2/F_2 mixing zone of their reactor. They did not identify which species in their active nitrogen was responsible for the IF excitation, but speculated that it might be $N_2(A\,^3\Sigma_u^+)$.

The present study examines the excitation of IF($B \rightarrow X$) emission in the electronic energy-transfer reaction between $N_2(A)$ and ground-state IF. Three types of measurements characterize fully the excitation of $IF(B\,^3\Pi_{0^+})$ by $N_2(A\,^3\Sigma_u^+)$. Spectral scans under a variety of conditions characterized the distribution of IF(B) vibrational levels excited in the energy-transfer reaction. Measurements of IF(B) intensities as a function of IF number density in the presence of known number densities of $N_2(A)$ determine the rate coefficient for the excitation of IF(B) by $N_2(A)$. Finally the rate coefficient for $N_2(A)$ removal by IF was determined by monitoring the disappearance of $N_2(A)$ as a function of added IF number density. The following sections describe these measurements in detail.

II. EXPERIMENTAL

The apparatus used in these measurements is a 2 in. flow tube pumped by a Leybold–Heraeus roots blower/forepump combination capable of producing linear velocities up to 5×10^3 cm s^{-1} at pressures of 1 Torr. The flow-tube design is modular (see Fig. 1), with separate source, reaction, and detection sections which are clamped together with O-ring joints. We have described it in various configurations previously.[12–14] The detection region is a rectangular stainless-steel block bored out internally to a 2 in. circular cross section and coated with Teflon® (Dupont Poly TFE #852-201) to retard surface recombination of atoms.[15–17] Use of a black primer prior to the Teflon® coating reduces scattered light inside the block significantly. The block has two sets of viewing positions each consisting of four circular ports on the four faces of the block. These circular ports accommodate vacuum-ultraviolet resonance lamps, VUV and visible monochromator interfaces, laser delivery side-arms, and a spatially filtered photomultiplier/interference filter combination.

The downstream observation position contains baffled side arms to allow entry and exit of a laser beam, and at right angles to these a filtered photomultiplier and a UV/visible monochromator interface. The filtered photomultiplier is for detecting laser-induced fluorescence (LIF), while the

 0021-9606/85/235602-08$02.10

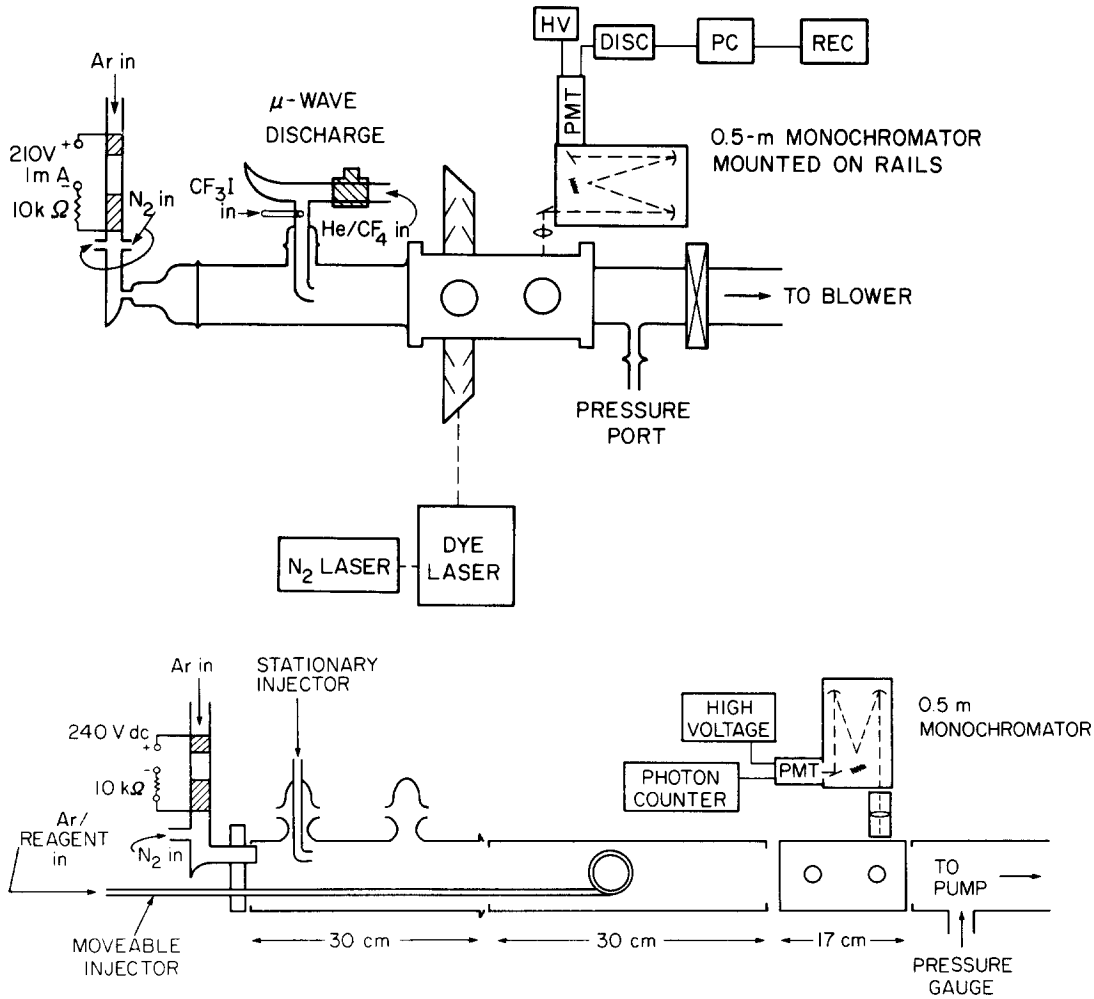

FIG. 1. (a) Flow-tube apparatus for studying $N_2(A)$ with IF. (b) Flow-tube apparatus configured for $N_2(A)$ decay-kinetics measurements.

monochromator is used in the bulk of these studies to detect fluorescence between 180 and 850 nm. A suprasil lens collects light from the center of the flow tube and focuses it on the entrance slit of a 0.5 m Minuteman monochromator outfitted with a 1200 groove mm^{-1} grating blazed at 250 nm. A thermoelectrically cooled photomultiplier detects photons with the aid of an SSR 1105 photon-counting rate meter and strip-chart recorder. Initial experiments used an EMI 9659QA photomultiplier (S-20 response), but for the last sets of measurements this was replaced by an HTV R943-02 photomultiplier (GaAs photocathode). This change resulted in significant improvements in red sensitivity, particularly beyond 650 nm.

The entire spectral detection network was calibrated for relative response as a function of wavelength using standard quartz-halogen (300 to 900 nm) and D_2 (180 to 400 nm) lamps. Absolute response calibrations were made *in situ* by observing the O/NO air afterglow under carefully controlled conditions using techniques we have documented previously.[12,18]

The reaction between metastable $Ar(^3P_{0,2})$ and molecular nitrogen produces the metastable nitrogren molecules, $N_2(A\ ^3\Sigma_u^+)$.[19,20] This transfer excites ground state N_2 to the $C\ ^3\Pi_u$ [21] state which quickly cascades radiatively to the metastable ($A\ ^3\Sigma_u^+$) via the $B\ ^3\Pi_g$ state. An aluminum-hollow-cathode discharge source operating at 240 V and 3 mA produced the argon metastables. Molecular nitrogen was mixed with the argon metastables just downstream of the discharge and observations of Vegard–Kaplan emission, $N_2(A\ ^3\Sigma_u^+ - X\ ^1\Sigma_g^+)$, are used to monitor the number density of the metastable nitrogen molecules. Figure 2 shows a spectrum of the Vegard–Kaplan bands in our reactor.

Reagents enter the flow tube through hook-shaped injectors whose outlet orifices are coaxial with the main flow tube. For some studies, reagents entered through a 1 in. diameter loop injector seated on the end of a 1/4 in diameter tube which slides along the bottom of the flow tube, parallel to its axis, thus allowing a variety of reaction distances to be achieved allowing accurate kinetic studies. The hook injectors facilitate introduction of unstable species produced in a secondary discharge. These injectors have relatively large diameters (10 mm) and are Teflon® coated to inhibit wall recombination of these unstable species. IF is produced in one of these injectors by the reaction between CF_3I and F atoms, the F atoms having been produced in a microwave discharge of He/CF_4 mixtures further upstream in the injector.

Because IF is known to be somewhat unstable with re-

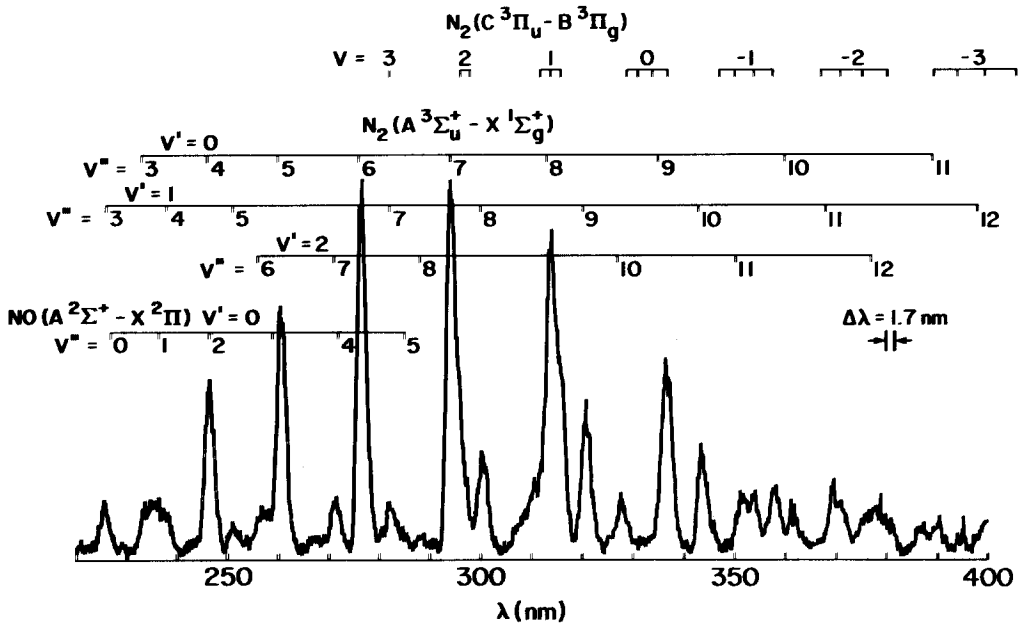

FIG. 2. Vegard–Kaplan emission in flow reactor 9 ms downstream from the discharge.

spect to wall reactions, we studied its production and loss in our flow system using a laser-induced fluorescence diagnostic for measuring IF number densities. Studies relating the production of F atoms to the residence time of CF_4 in the microwave discharge indicated a yield of about 0.3 F atoms per CF_4 molecule under typical operating conditions. We determined experimentally conditions that produce complete reaction of CF_3I in the injector and showed that a negligible amount of IF is destroyed in the injector under these conditions. At low flow velocities wall collisions do destroy some of the IF molecules in the main flow tube, presumably on the non-Teflon coated windows. This loss appears to be negligible at higher velocities, however, and permits us to operate in a regime where IF number densities may be related directly to the amount of CF_3I flowing into the injector when F atoms are in excess. This is fortunate because operating the injector using excess CF_3I results in the deposition of an optically opaque thin film on the reactor walls.

Mass-flow meters or rotameters monitor the flow rates of most gases. All flow meters were calibrated by measuring rates of increase of pressure with time into 6.5 or 12 ℓ flasks, using appropriate differential pressure transducers (Validyne DP-15) which themselves have been calibrated with silicon oil or mercury manometers. Typical flow rates for argon, nitrogen, and helium through the injector are 2000–5000, 100–500, and 200–500 μmole s^{-1}, while CF_4 and CF_3I flow rates range between 0 and 1 μmole s^{-1}, respectively. Total pressures, as measured by a Baratron® capacitance manometer, range from 0.4 to 9 Torr, and flow velocities vary from 500 to 5000 cm s^{-1} as controlled by a variable-conductance butterfly valve.

Tetrafluoromethane (CF_4) was obtained 99.5% pure from Matheson, and, due to the small amount employed, was used without further purification. Trifluoroiodomethane (CF_3I) was obtained 99% pure from PCR Research Chemicals. The major impurity, I_2, was removed by distilling CF_3I from a trap at -115 °C followed by storage in a dark bulb. The other gases, Ar, N_2, and He, were taken directly from their cylinders but flowed through molecular sieve traps before entering the reactor.

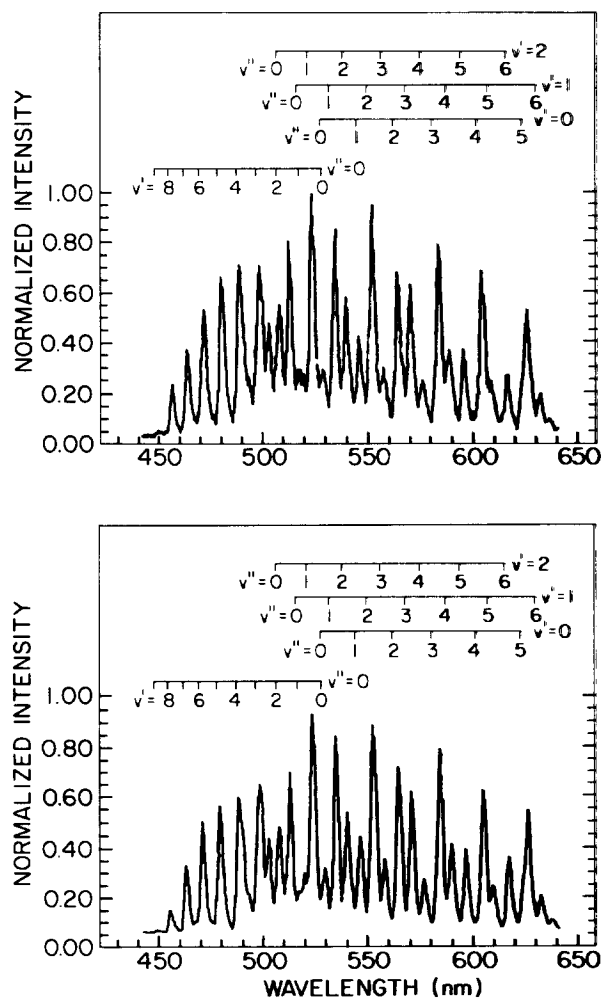

FIG. 3. Experimental (top) and computed (bottom) IF(B) spectra from $N_2(A)$ excitation of IF at 0.5 Torr.

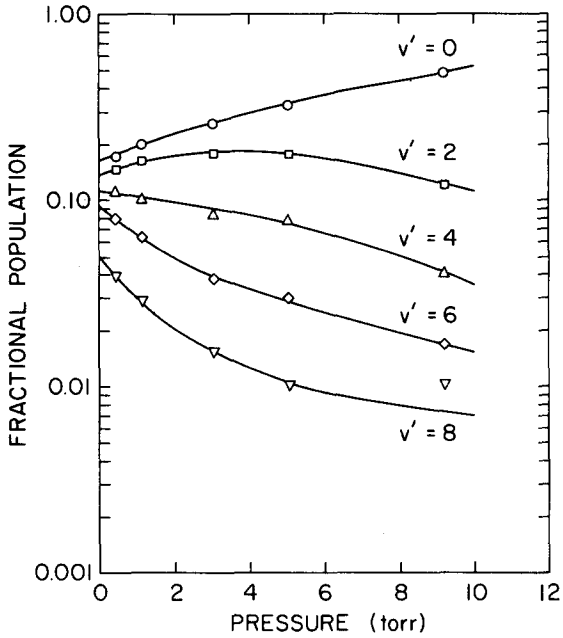

FIG. 4. IF($B\,^3\Pi_0^+$) populations from $N_2(A\,^3\Sigma_u^+\, v'=0)$ + IF(X).

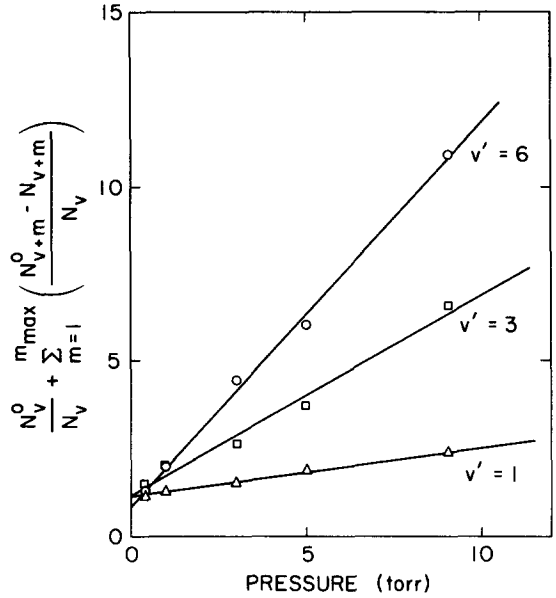

FIG. 5. Stern–Volmer plots for IF(B) vibrational relaxation in 80/20, Ar/N_2–He mixtures.

III. RESULTS AND ANALYSIS

A. Vibrational distributions from $N_2(A)$ excitation

When IF is added to a flow of $N_2(A)$ metastables, the IF($B\,^3\Pi_{0^+}$–$X\,^1\Sigma^+$) system radiates prominently in the spectral region between 440 and 640 nm. Figure 3 shows a typical spectrum. Relative populations of the B-state vibrational levels were determined by dividing the response-corrected, wavelength-integrated intensity of a given band by the appropriate Einstein emission-rate coefficient.[22] The band intensities were determined either by planimetry or by a least squares spectral fitting analysis. The spectral analysis consists of a linear least squares fit between the observed spectrum and a computed spectrum to determine number densitites of the emitting states. The computed spectra are determined from the appropriate spectroscopic constants[23(a)] by calculating the line-by-line, intensity-weighted spectral distributions for each transition at an assumed rotational temperature (usually ambient), convolving with the experimental scanning function, and solving for the set of upper-state populations which permit the best least squares fit to the experimental observations. This procedure allows us to account quantitatively for unresolved overlap between adjacent spectral features. The integrated band transition probabilities were determined from a complete reanalysis of the RKR potentials, Franck–Condon factors, and the transition moment function as described elsewhere.[22] The values thus derived are consistent with those obtained from the data of Trautman *et al.*[23(b)] The lower portion of Fig. 3 shows a typical synthetic fit. Figure 4 shows how the vibrational population distribution varies with pressure over the range of 0.5 to 9 Torr. The increase in population of the lower vibrational levels and the concomitant decrease in population of the upper vibrational levels demonstrates graphically the extent of vibrational relaxation.

A modified Stern-Volmer analysis of the data in Fig. 4 allows us to estimate vibrational relaxation coefficients. The analysis assumes that vibrational relaxation proceeds only a single quantum at a time and that the gas composition is constant. Our mixture is approximately 80% argon and 20% helium and nitrogen, with minor amounts of CF_4 added for this series of experiments. The CF_4 rapidly relaxes the $N_2(A)$ vibrational distribution to $v'=0$. Wolf *et al.* have shown that electronic quenching of IF(B) by Ar, N_2, and He is negligible.[24]

Because its radiative decay rate is rapid compared to the rate of removal of species from the field of view by physical transport, the IF* is in steady state in the observation region. Thus in the absence of vibrational relaxation we have

$$R_v = N_v^0 A_v, \tag{1}$$

where R_v is the rate of formation of IF(B) in vibrational level v, N_v^0 is the population of that level, and A_v is the radiative decay rate. When vibrational relaxation is included, Eq. (1) becomes

$$R_v + k_{v+1,v} N_{v+1} \frac{PN_0}{RT} = (A_v + k_{v,v-1} \frac{PN_0}{RT}) N_v, \tag{2}$$

where $k_{v,v-1}$ represents the vibrational relaxation rate out of level v, $k_{v+1,v}$ the vibrational relaxation rate coefficient into level v, P the gas pressure, N_0 Avogadro's number, R the gas constant, and T the temperature. Summing Eqs. (1) and (2) over all levels above level v, subtracting the resultant sums of Eq. (1) from Eq. (2), and dividing through by the quantity $N_v A_v$, gives the working equation for the vibrational-relaxation analysis:

$$\frac{N_v^0}{N_v} + \sum_{m=1}^{m} {}^{\max}\left(\frac{N_{v+m}^0 - N_{v+m}}{N_v}\right) = 1 + \frac{k_{v,v-1}}{A_v}\frac{N_0}{RT} P. \tag{3}$$

Figure 5 shows some typical plots of the data analyzed according to Eq. (3). Least-squares fits to the data for each

TABLE I. Rate coefficients for vibrational relaxation of IF($B\,^3\Pi_0^+$) by an 80/20 Ar/He–N_2 Mixture.

v'	$k^{a,b}_{v,v-1}$
1	0.6
2	1.6
3	2.6
4	3.5
5	2.6
6	4.1
7	4.0
8	2.9

[a] Units of 10^{-12} cm^3 molecule^{-1} s^{-1}.
[b] Uncertainty estimated to be 30%.

vibrational level indicate that the vibrational relaxation rate coefficients range from 2.6 to 4×10^{-12} cm^3 molecules^{-1} s^{-1} for vibrational levels 3–8. Levels 1 and 2 relax a bit more slowly with rate coefficients of 0.6 and 1.6×10^{-12} cm^3 molecule^{-1} s^{-1}, respectively. Table I summarizes the vibrational-relaxation-rate measurements. Experiments at the Air Force Weapons Laboratories[24(b)] have indicated that the rate coefficients for vibrational relaxation of $IF(B)_{v'=3}$ by helium, nitrogen, and argon are 5.7, 3.9, and 1.2×10^{-12} cm^3 molecule^{-1} s^{-1}, respectively. From these data we calculate a vibrational relaxation rate coefficient for an 80/20 Ar/N_2–He mixture (with an average rate coefficient for the He–N_2 component of 5×10^{-12} cm^3 molecule^{-1} s^{-1}) of 2.0×10^{-12} cm^3 molecule^{-1} s^{-1} which agrees well with our measured value of 2.6×10^{-12} cm^3 molecule^{-1} s^{-1} given the 30% to 40% uncertainty in the AFWL data, and our own experimental uncertainties which must be of comparable size. The AFWL experiments also indicate that the rate coefficients for relaxation of vibrational level 1 by He, Ne, and N_2 are about a factor of 3 smaller than the corresponding rate coefficients for vibrational level 3. This agrees well with the factor of 4 reduction observed in our experiments.

B. Rate coefficients for the excitation of IF($B\,^3\Pi_{0^+}$) by $N_2(A\,^3\Sigma_u^+)$

Knowledge of the vibrational distribution of the B-state emission, and measurements of the change in intensity of various bands as a function of IF number density, for otherwise constant conditions, determines the rate coefficient for excitation of IF by collisions with $N_2(A)$. The differential equation describing the rate of change in the IF(B) number density with time is

$$\frac{d[IF^*]}{dt} = k_{ex}[IF][N_2(A)] - k_{rad}[IF^*], \tag{4}$$

where k_{ex} is the rate coefficient for IF(B) excitation by $N_2(A)$ and k_{rad} is the radiative decay rate of IF*. We have ignored electronic quenching of the IF(B) state by the various species in the reactor.[24] Because the IF(B) radiative-decay rate is quite large, the IF(B) is in steady state in the observation volume. Thus its intensity is

$$I_{IF*} = k_{rad}[IF^*] = k_{ex}[IF][N_2(A)] = k_{ex}[IF]\frac{I_{N_2(A)}}{A_{N_2(A)}}, \tag{5}$$

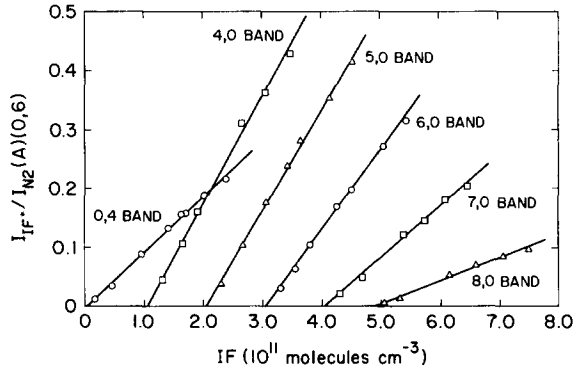

FIG. 6. Variation in the ratio of IF($B\,^3\Pi_0^+$) intensity to that for the 0,6 Vegard–Kaplan band as a function of IF number density. Abscissa offsets applied for clarity.

where $I_{N_2(A)}$ and $A_{N_2(A)}$ are the intensity and transition probability of $N_2(A)$ in the observation volume. This expression can be rearranged to give

$$\frac{I_{IF*}}{I_{N_2(A)}} = \frac{k_{ex}[IF]}{A_{N_2(A)}}. \tag{6}$$

Equation (6) shows that the ratio of the intensity of IF(B) to that for $N_2(A)$ should vary linearly with IF number density. Figure 6 shows that this is indeed the case for a number of different vibrational levels of the IF(B) state.

The experimental runs monitored only the intensities of the peak heights of the Vegard–Kaplan or IF(B) bands. Planimetry or numerical integration determined the ratio of band areas to peak heights which were the required correction factors in analyzing the raw data. Dividing the integrated band areas of a given v',v'' band by branching ratios determined from our IF(B) Einstein-coefficient calculations[22] gave the total emission intensity out of a given vibrational level of the IF(B) electronic state. Dividing this $IF(B)_{v'}$ intensity by the fraction of the total IF(B) population in a given v' state gave the total fluorescence from all vibrational levels of the IF($B\,^3\Pi_{0^+}$) state. Shemansky's Einstein coefficients,[25] weighted appropriately for the lifetime differences of the degenerate sublevels of the $N_2(A)$ state, were used to convert the Vegard–Kaplan emission intensities to $N_2(A)$ number densities. A number of different runs at 1 Torr total pressure showed that the total rate coefficient for IF(B) excitation into all vibrational levels in the energy-transfer reaction between $N_2(A)$ and IF(X) is $(0.83\pm0.10)\times10^{-10}$ cm^3 molecule^{-1} s^{-1}. This value is independent of which band is being observed, the transit times from the injector to the observation volume (less than $\approx$10 ms), and the initial F-atom number density.

A few excitation-rate-coefficient measurements at higher pressures indicated an apparent decrease in the excitation rate coefficient with increasing pressure. The drop was about a factor of 2 between 1 and 5 Torr. We think the reduction in apparent IF excitation rates at higher pressures results from overestimating IF number densities because IF losses on the reactor walls during the longer transit times from the injector to the detector, which accompanied the high pressure studies, were not included in the analysis. Any real electronic quenching in our system represents only a minor loss.

The ratio of total IF fluorescence intensity to $N_2(A)$ number density in the presence of 2% CF_4 added to the bath gas just downstream of the metastable discharge indicated a roughly 20% decrease in the IF fluorescence from the intensities observed in the absence of CF_4. The CF_4 relaxes the $N_2(A)$ vibrational levels, so that in its presence, only $N_2(A\ v'=0)$ is in the reactor. Thus the implication of this observation is that the excitation-rate coefficient is slightly smaller for $N_2(A\ v'=0)$ than it is for higher levels of $N_2(A)$. We do not feel confident in this assertion, however, because adding the CF_4 also causes the IF(B) distribution to be vibrationally relaxed and any error in relative monochromator response function or IF(B) transition probabilities will be reflected in the total IF fluorescence intensity measurement. Thus we can state with confidence only that no dramatic changes occur when the $N_2(A)$ is vibrationally relaxed compared to conditions under which it is not. The rate coefficients for $N_2(A)$ removal by IF do not show any dependence on $N_2(A)$ vibrational energy (see below).

C. Rate coefficients for $N_2(A)$ removal by IF and other molecules

For these experiments the important kinetic processes in our reactor which involve $N_2(A)$ are:

$$N_2(A) + IF \rightarrow N_2(X) + IF^* \quad (7a)$$

$$\rightarrow \text{other products}, \quad (7b)$$

$$N_2(A) + Q \rightarrow N_2(X) + Q', \quad (8)$$

$$N_2(A) + \text{wall} \rightarrow N_2(X), \quad (9)$$

where Q represents other quenchers. Given these reactions, the differential equation describing the variation in the $N_2(A)$ number density with time is

$$\frac{d[N_2(A)]}{dt} = -\{k_7[IF] + k_8[Q] + k_9\}[N_2(A)]. \quad (10)$$

Because IF any any other significant quenchers in the reactor will be at much greater number densities than $N_2(A)$, they can be considered to be constant (the pseudo-first-order approximation) and the differential equation can be solved to give

$$\ln\left\{\frac{[N_2(A)]_t}{[N_2(A)]_{(t=0)}}\right\} = -\{k_7[IF] + k_8[Q] + k_9\}t, \quad (11)$$

where the reaction time t in the flow reactor is given by the ratio of the distance between the injector and the detection region z and the bulk flow velocity $\bar{v}$. For fixed z and $\bar{v}$ (fixed-injection-port analysis), measurements of the change in $N_2(A)$ number density as a function of reagent number density give a decay coefficient Γ,

$$\Gamma = -\frac{d \ln I_{N_2(A)}}{d[Q]} = k_8[Q]z/\bar{v}, \quad (12)$$

given that the $N_2(A)$ number density is directly proportional to the Vegard–Kaplan emission intensity. The desired rate coefficient then is the ratio of the slope of a plot of $\ln I_{N_2(A)}$ vs [Q], i.e., Γ, to the reaction time $z/\bar{v}$.

The above analysis assumes perfect mixing at the injector, and neglects the fluid dynamic effects of the coupling of the radial density gradient of the $N_2(A)$ (it is destroyed with unit efficiency in collisions with the walls) with a radial velocity profile. This latter effect has been thoroughly discussed in the literature[26–33] with the result that under appropriate conditions $d \ln I_{VK}/d[IF] = -0.62\, k_7 z/\bar{v}$. These conditions are generally obtained in our experiments.

The correction for imperfect mixing must be made empirically by doing experiments at several different values of z. Then the effective mixing length, $z_{eff} = z - z_0$ is deduced by plotting decay coefficients Γ as a function of reaction time and extrapolating to zero reaction time.

We observed the decays in the log of the Vegard–Kaplan intensity as a function of the number densities of IF, CF_3I, CF_4, and NF_3 for both vibrational levels 0 and 1 of $N_2(A)$ and CF_3H, CH_4, and SF_6 for vibrational level 1. We made careful measurements of the CF_3I quenching rate coefficient at three different mixing distances, and applied the mixing correction so obtained to the results of the other systems.

Figure 7 shows the decay in the (0,6) Vegard–Kaplan intensity as a function of CF_3I number density for three diferent reaction times. The slopes of the decays in Fig. 7 are

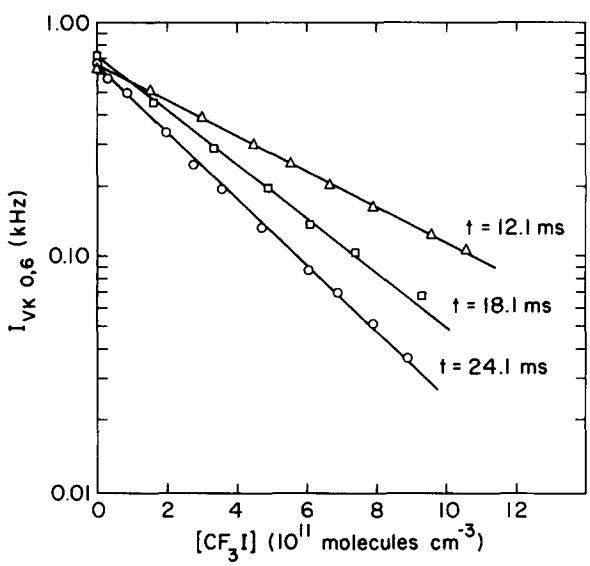

FIG. 7. The decay of the Vegard–Kaplan bands as a function of CF_3I number density for three different reaction times.

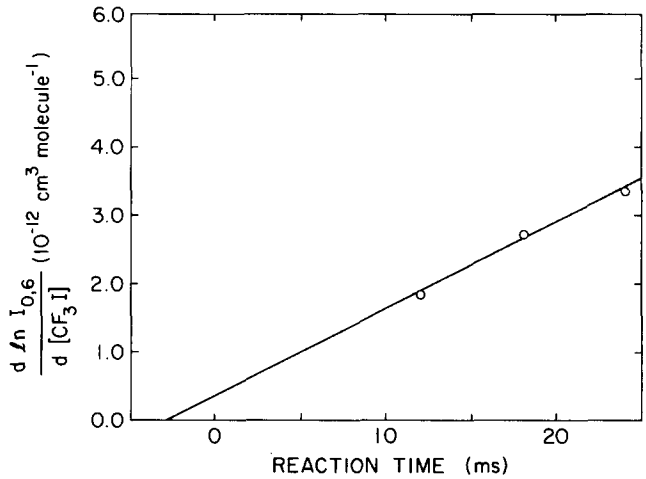

FIG. 8. Variation in Vegard–Kaplan decay rates with CF_3I as a function of reaction time.

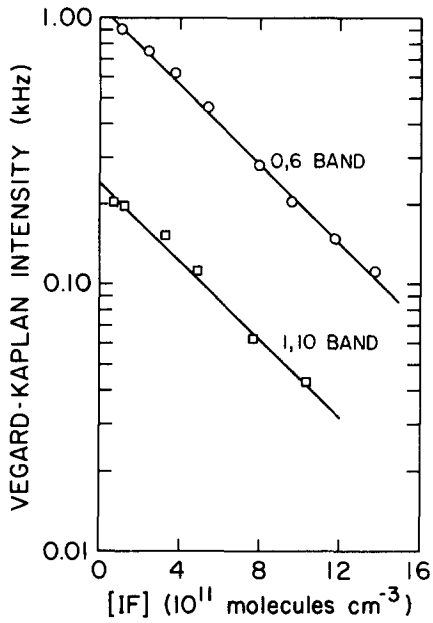

FIG. 9. Decay of the intensity of the Vegard–Kaplan bands as a function of IF number density.

plotted against reaction time in Fig. 8 to determine a mixing correction to the data. These results and similar data for $v' = 1$ indicate that CF_3I quenches $N_2(A)$ with rate coefficients of 2.0 and 2.1×10^{-10} cm^3 $molecule^{-1}$ s^{-1} for vibrational levels 0 and 1, respectively. Because the accuracy of these determinations is only about 15%, the difference in the coefficients for the two levels is not significant.

Figure 9 shows the decay of $N_2(A)$ as a function of IF number density. These data coupled with runs under different sets of conditions indicate that the rate coefficient for removal of $N_2(A)$ by IF is 1.9 and 2.0×10^{-10} cm^3 $molecule^{-1}$ s^{-1} for vibrational levels 0 and 1 of $N_2(A)$, respectively. Again the 5% difference between the coefficients for the two different levels is much smaller than the overall 15% uncertainty in the measurements.

Table II summarizes all quenching-rate coefficient determinations. The measurements on IF and CF_3I were carefully done and carry an overall uncertainty (statistical plus systematic) of 15%. The measurements on CF_4, CF_3H, CH_4, NF_3, and SF_6 were survey measurements of potential vibrational relaxation partners for $N_2(A\ v' > 0)$, and are therefore only accurate to a factor of 2.

IV. DISCUSSION

The rate coefficients for vibrational relaxation of $N_2(A,v' = 1)$ by CF_4 and CH_4 agree reasonably well with the results of the more detailed studies of Jeffries *et al.*[34] ($k_{CF_4} = 4.7\times10^{-13}$ cm^3 $molecule^{-1}$ s^{-1}, $k_{CH_4} = 15\times10^{-13}$ cm^3 $molecule^{-1}$ s^{-1}) and of Clark and Setser[35] ($k_{CH_4} = 11\times10^{-13}$ cm $molecule^{-1}$ s^{-1}). To our knowledge, our measurements are the first reports of any of the other rate coefficients in Table II. In their laser-induced fluorescence studies on $N_2(A,v' = 0)$, Heidner *et al.*[36] inferred that SF_6 relaxed $N_2(A)$ vibrational energy. Our experiments indicate that this is true, but that the efficiency for relaxation by SF_6 is extremely low.

Cao and Setser[37] have studied the quenching of $N_2(A)$ by the halogen molecules Cl_2, Br_2, I_2, ICl, and IBr. Like IF, they all quench $N_2(A)$ very rapidly with rate coefficients between 1 and 2×10^{-10} cm^3 $molecule^{-1}$ s^{-1}. IF appears to be the only halogen species, however, that fluoresces strongly when excited by $N_2(A)$ molecules. Cao and Setser did observe some weak fluorescence when I_2 was excited by $N_2(A)$, (< 1% of total quenching). Coombe and Lam[38] observed weak $Br_2[D'\,^3\Pi(2_g)$–$A'\,^3\Pi(2u)]$ fluorescence which they attributed to arise from the interaction of $N_2(A)$ with Br_2, again < 1% of total quenching. Cao and Setser failed to observe any fluorescence from Br_2 when they mixed it with $N_2(A)$.

The very strong excitation of IF by $N_2(A)$, in the absence of any significant excitation of other halogens by $N_2(A)$ is somewhat surprising. If the coupling of entrance to exit channels is direct, then the energy defect will be approximately 3.5 eV, enough to leave the product ground-electronic-state nitrogen with 14 quanta of vibrational energy. Large energy defects in efficient $N_2(A)$ transfer reactions are not all that unusual, the energy defect for $O(^1S)$ excitation in the $N_2(A)$ + O reaction being 2 eV, for example.[39] The efficacy of such reactions is aided, presumably, by the large Franck–Condon factors involved in $N_2(A)$ transitions on the order of 4 eV. Deperasinska *et al.*[40] have shown that Franck–Condon overlap appears to be one of the contributing features in an efficient intermolecular electronic energy-trans-

TABLE II. $N_2(A)$ Rate coefficient determinations.

Reaction	Rate coefficient (cm^3 $molecule^{-1}$ s^{-1})	
$N_2(A,v' = 0,1) + IF \rightarrow IF(B\,^3\Pi_{0^+}) + N_2(X)$	0.83×10^{-10}	
$N_2(A) + IF \rightarrow$ products	1.9×10^{-10}	$v' = 0$
	2.0×10^{-10}	$v' = 1$
$N_2(A) + CF_3I \rightarrow$ products	2.0×10^{-10}	$v' = 0$
	2.1×10^{-10}	$v' = 1$
$N_2(A,v' = 1) + CF_4 \rightarrow N_2(A,v' = 0) + CF_4$	3×10^{-13}	
$N_2(A,v' = 0) + CF_4 \rightarrow N_2(X) + CF_4$	$< 10^{-14}$	
$N_2(A,v' = 1) + CF_3H \rightarrow N_2(A,v' = 0) + CF_3H$	9×10^{-13}	
$N_2(A,v' = 1) + CH_4 \rightarrow N_2(A,v' = 0) + CH_4$	14×10^{-13}	
$N_2(A) + NF_3 \rightarrow$ products	3×10^{-13}	$v' = 0$
	9×10^{-13}	$v' = 1$
$N_2(A,v' = 1) + SF_6 \rightarrow N_2(A,v' = 0) + SF_6$	1×10^{-14}	

fer reaction. The even larger energy-defect transition in the $N_2(A) + IF$ interaction occurs, however, with a rather small Franck–Condon overlap, so that one might not expect direct energy transfer in to the $B\ ^3\Pi_{0^+}$ state of IF to be important. The Franck–Condon factors for IF(B) excitation are large, however, and the Franck–Condon factors of both the donor and acceptor species are important in Deperasinska *et al.* formalism. Furthermore, the long-lived complex indicated by the broad distribution of product states and the polar nature of IF may distort the $N_2(A)$ wave function thereby enhancing the larger energy-defect Franck–Condon factors.

An alternative scheme is that the direct energy transfer is into an intermediate IF state which is coupled radiatively to the $^3\Pi_{0^+}$ state. We saw no emission in our reactor between 200 and 850 nm that could not be attributed to either $N_2(A)$ or IF(B). If the acceptor state of IF were to lie around 4.5 eV however, its radiative transition to the B state would lie too far into the red to be observed by our detection system.

The $D'\ ^3\Pi_2 g$ state of IF lies about 4.7 eV above the ground state and the strong D'–A transition falls in the region between 450 and 500 nm. We saw no features in this spectral region that could be ascribed to this transition, and conclude that any excitation of the D' state of IF by $N_2(A)$ must be at least two orders of magnitude less efficient than the excitation of the B state. This is consistent with Coombe and Lam's report of Br_2 D' excitation by $N_2(A)$ which they said proceeded with a rate coefficient of only 1×10^{-13} cm^3 $molecule^{-1}$ s^{-1}.

ACKNOWLEDGMENTS

We appreciate illuminating discussions with George Caledonia and Paul Lewis (PSI) and Don Setser (Kansas State University) and technical assistance from Henry Murphy and Megan Donahue. We are grateful for support from the Air Force Weapons Laboratories under contract F29601-83-C-0051.

[1] J. G. Eden, M. L. Dlabal, and S. B. Hutchinson, IEEE J. Quantum Electron. **QE-17**, 1085 (1981).
[2] M. A. A. Clyne and I. S. McDermid, J. Chem. Soc. Faraday Trans. 2 **74**, 644 (1978).
[3] M. A. A. Clyne and I. S. McDermid, J. Chem. Soc. Faraday Trans. 2 **74**, 664 (1978).
[4] M. A. A. Clyne and I. S. McDermid, J. Chem. Soc. Faraday Trans. 2 **74**, 1376 (1978).
[5] M. A. A. Clyne and I. S. McDermid, J. Chem. Soc. Faraday Trans. 2 **74**, 1644 (1978).
[6] M. A. A. Clyne, M. C. Heaven, and E. Martinez, J. Chem. Soc. Faraday Trans. 2 **76**, 177 (1980).
[7] M. A. A. Clyne and J. P. Liddy, J. Chem. Soc. Faraday Trans. 2 **76**, 1569 (1980).
[8] (a) S. J. Davis and L. Hanko, Appl. Phys. Lett. **37**, 692 (1980); (b) S. J. Davis, L. Hanko, and R. F. Shea, J. Chem. Phys. **78**, 172 (1983).
[9] M. A. A. Clyne, J. A. Coxon, and L. W. Townsend, J. Chem. Soc. Faraday Trans. 2 **68**, 2134 (1972).
[10] P. D. Whitefield, R. F. Shea, and S. J. Davis, J. Chem. Phys. **78**, 6793 (1983).
[11] S. J. Davis (private communication, 1983).
[12] W. T. Rawlins, L. G. Piper, G. E. Caledonia, and B. D. Green, Physical Sciences Inc. Technical Report, TR-298, 1981. Available from the authors upon request.
[13] L. G. Piper, G. E. Caledonia, and J. P. Kennealy, J. Chem. Phys. **74**, 2888 (1981).
[14] W. T. Rawlins and L. G. Piper, Proc. Soc. Photo-Opt. Instrum. Eng. **279**, 58 (1981). Also presented at the Technical Symposium East '81 of the Society of Photo-Optical Instrumentation Engineers, Washington, D. C. (April, 1981).
[15] R. H. Krech, G. J. Diebold, and D. L. McFadden, J. Am. Chem. Soc. **99**, 4605 (1977).
[16] M. Kaufman and C. E. Kolb, NR 092-531, 8 (1971).
[17] H. C. Berg and D. Kleppner, Rev. Sci. Instrum. **33**, 248 (1962).
[18] L. G. Piper, G. E. Caledonia, and J. P. Kennealy, J. Chem. Phys. **75**, 2847 (1981).
[19] D. W. Setser, D. H. Stedman, and J. A. Coxon, J. Chem. Phys. **53**, 1004 (1970).
[20] D. H. Stedman and D. W. Setser, Chem. Phys. Lett **2**, 542 (1968).
[21] N. Sadeghi and D. W. Setser, Chem. Phys. Lett. **82**, 44 (1981).
[22] W. J. Marinelli and L. G. Piper, J. Quant. Spectrosc. Radiat. Transfer (to be published).
[23] (a) A. Trickl and J. Wanner, J. Mol. Spectrosc. **104**, 174 (1984); (b) M. Trautman, J. Wanner, S. K. Zhou, and C. R. Vidal, J. Chem. Phys. **82**, 693 (1985).
[24] (a) P. J. Wolf, J. H. Glover, L. Hanko, R. F. Shea, and S. J. Davis, J. Chem. Phys. **82**, 2321 (1985); (b) P. J. Wolf (private communication, 1984); (c) P. J. Wolf and S. J. Davis, J. Chem. Phys. **83**, 91 (1985).
[25] D. E. Shemansky, J. Chem. Phys. **51**, 689 (1969).
[26] E. E. Ferguson, F. C. Fehsenfeld, and A. L. Schmeltekopf, *Advances in Atomic and Molecular Physics V*, edited by D. R. Bates (Academic, New York, 1970).
[27] R. C. Bolden, R. W. Hemsworth, M. J. Shaw, and N. D. Twiddy, J. Phys. B **3**, 45 (1970).
[28] A. L. Farragher, Trans. Faraday Soc. **66**, 1411 (1970).
[29] R. W. Huggins and J. H. Cahn, J. Appl. Phys. **38**, 180 (1967).
[30] R. E. Walker, Phys. Fluids **4**, 1211 (1961).
[31] R. V. Poirier and R. W. Carr, J. Phys. Chem. **75**, 1593 (1971).
[32] M. Cher and C. S. Hollingsworth, Adv. Chem. Ser. **80**, 118 (1969).
[33] J. H. Kolts and D. W. Setser, J. Chem. Phys. **68**, 4848 (1978).
[34] J. M. Thomas, J. B. Jeffries, and F. Kaufman, Chem. Phys. Lett. **102**, 50 (1983).
[35] W. G. Clark and D. W. Setser, J. Phys. Chem. **84**, 2225 (1980).
[36] R. F. Heidner, III, D. G. Sutton, and S. H. Suchard, Chem. Phys. Lett. **37**, 2431 (1976).
[37] D. -Z. Cao and D. W. Setser, Chem. Phys. Lett. **116**, 363 (1985).
[38] R. D. Coombe and C. H. -T. Lam, J. Chem. Phys. **80**, 3106 (1984).
[39] L. G. Piper, J. Chem. Phys. **77**, 2373 (1982).
[40] I. Deperasinska, J. A. Beswick, and A. Tramer, J. Chem. Phys. **71**, 2477 (1979).